

Airflow Simulation inside Reefer Containers

Safir Issa^{1,2}, Walter Lang^{1,2}

¹IMSAS (Institute for Microsensors, Actuators and Systems), Microsystems Center Bremen (MCB), University of Bremen, Otto-Hahn-Allee, Bld. NW1, D-28359 Bremen, Germany

²IGS (International Graduate School for Dynamics in Logistics), University of Bremen, c/o BIBA Hochschulring 20, D-28359 Bremen, Germany;

{sissa, wlang}@imsas.uni-bremen.de

Abstract Transporting of sensitive commodities in strict ambient conditions becomes necessity not only to fulfill regulations but also to maintain their quality and to reduce the losses rate. Temperature, which is mainly affects the transported produce, is controlled by airflow pattern in reefer containers. Consequently, obtaining airflow pattern enables predicting hot spots and then taking the necessary actions to minimize their effects. We present in this paper, a k- ϵ simulation model to evaluate airflow pattern in reefer container loaded with bananas. Simulation results predict the place of the hot spots. Moreover, we found that the cooling distribution is improved by modification of the scheme for placing pallets in the container, the so called chimney layout.

Keywords Characterization, Airflow, k- ϵ simulation, Banana transport, Reefer container

1 Introduction

Nowadays, the “fresh” agriculture products are available in markets almost all over the year due to the huge progress in logistic transport. Nevertheless, the intercontinental transport of sensitive products, such as banana, still has serious challenges to maintain the quality of these products. Banana, as an example, is a sensitive product that is highly affected by surrounding environments. Its optimum temperature for transport and storage is 13-14 °C (Paull, 1999). Higher temperatures may speed up the ripening process or cause the senescence, whereas lower temperatures may cause freezing or chilling injury. Therefore, it is essential to have uniform temperatures throughout the system to maintain commodities quality and shelf life during transportation processes. Obtaining homogeneous air distribution is extremely complex matter due to operational factors such as loading practices and product properties (Smale et al., 2006). In reefer containers convection is the dominant mode of heat transfer; therefore, the temperature and its dis-

tribution are governed by airflow pattern (Moureh et al., 2009). Distributed airflow is responsible of removing generated heat not only from container's walls and doors caused by external heat sources, but also the heat generated by the commodities themselves. Fruits keep producing heat and moisture after harvesting. In some regions of the transport container, where ventilation is poor, hot spots start to be created. As a consequence, commodities in these stagnant zones are object to different deteriorations that degrade their quality. Hot spots can emerge in different areas of the container. The difficulties to predict their location and development (Jedermann et al., 2013) cause a major problem for the supervision of banana transports. In order to understand flow behavior in such enclosed areas, researchers have been developing airflow models in the last four decades. With the new powerful computers, Computational Fluid Dynamics (CFD) became their preferred choice. Such numerical models, regarding their advantages of fast time and low cost, offer a powerful tool to understand fluid flow and heat transfer in the intended enclosed environments.

Zou et al. (2005) developed a CFD modeling system of the airflow patterns and heat transfer inside ventilated apple package through forced air cooling. The model was validated by temperature measurements of products, but this model is concerned by food packages and not the whole container. Moureh et al. (2009) presented a numerical approach and experimental characterization of airflow within a semi-trailer enclosure loaded with pallets in a refrigerated vehicle with and without air ducts. Measurements of air velocities were carried out by a laser Doppler velocimeter in clear regions (above the pallets) and thermal sphere-shaped probes located inside the pallets. The velocimeter is placed outside the vehicle and the measurement is done through a glass window. Results showed the importance of narrow spaces around pallets to reduce temperature variability in the truck, in addition to the fact of using air-ducts which improves the ventilation homogeneity. Xie et al. (2006) presented a CFD model which studies the effect of design parameters on flow and temperature field of a cold store. Many other CFD studies were reported.

In Section 2, we present CFD simulations of air flow pattern inside a container loaded with pallets. The simulations were done by using the $k-\epsilon$ model of the COMSOL Multiphysics software. Locations with low airflow, which are prone to develop hotspots, are identified by the simulations. Because the size of banana pallets does not fit the container dimensions, part of the pallets have to be rotated by 90° . The effect of a new scheme for loading the pallets to the container to the equability of the airflow was verified by the simulation. In Section 3, we validate the simulation results by comparison with the result of experimental test. Finally, we summarize the founded results by the achieved work.

2 Simulation Model

The CFD is used to determine airflow distributions by solving a set of equations describing the fluid motion and energy conservation. CFD predicts turbulent flows through three basic approaches: Direct numerical Simulation (DNS), Large-Eddy Simulation (LES), and Reynolds-Averaged Navier-Stokes (RANS) equations. Firstly, DNS solves Navier-Stokes equations without approximation for the whole range of spatial and temporal scales of the turbulence. Consequentially, DNS requires a very fine grid resolution and very small time steps which leads to an extremely long simulation (Nieuwstadt, 1994). Secondly, LES corresponds to the three-dimensional, time-dependent equations with the approximation of eliminating the very fine spatial grid and small time step. This consideration comes from the fact that macroscopic structure is characteristic for turbulent flow. Moreover, the large scales of motion are responsible for all transport processes. LES are still need a considerable computing time but in the other side gives detailed information on airflow turbulence (Zhai, 2007). Thirdly, RANS equations with turbulence models deal with the mean of the air parameters, which is more useful than the instantaneous value of the turbulent flow parameters. As a consequence airflow distributions can be quickly predicted. The RANS approach evaluate Reynolds-averaged variables for both steady-state and dynamic flows. The k-ε model is one of the most common turbulence models belonging to this approach. It is a two equation model i.e. it includes two extra transport equations to represent the turbulent properties of the flow. Due to its smaller requirements of computer resources, RANS approach has become very popular in modeling airflow in enclosed environments (Zhai, 2007). The Reynolds-averaged Navier-Stokes equations are given as:

$$\frac{\partial U_i}{\partial t} + U_j \frac{\partial U_i}{\partial x_j} = -\frac{1}{\rho} \frac{\partial P}{\partial x_i} + \frac{\partial}{\partial x_j} \left[\frac{(\mu + \mu_t)}{\rho} \frac{\partial U_i}{\partial x_j} \right] \quad (1)$$

$$\frac{\partial U_i}{\partial x_i} = 0 \quad (2)$$

where U_i is the mean velocity of the i -th component of fluid velocity (u) at the point of space (x) and at the time (t); P is the mean static pressure; ρ is the mean fluid density; μ is the dynamic viscosity; and μ_t is the turbulent eddy viscosity defined by Boussinesq relationship:

$$-\overline{u'_i u'_j} = 2 \frac{\mu_t}{\rho} S_{ij} \quad (3)$$

where $\overline{u'_i u'_j}$ is the Reynolds stress and S_{ij} is the mean strain rate given as:

$$S_{ij} = \frac{1}{2} \left(\frac{\partial U_i}{\partial x_j} + \frac{\partial U_j}{\partial x_i} \right) \quad (4)$$

The two equations for k- ϵ model are the kinetic turbulent energy (k) equation and the turbulent dissipation rate (ϵ) equation. They are given as:

$$\frac{\partial k}{\partial t} + U_j \frac{\partial k}{\partial x_j} = \frac{\mu_t}{\rho} S^2 - \epsilon + \frac{\partial}{\partial x_j} \left[\frac{1}{\rho} \left(\mu + \frac{\mu_t}{\sigma_k} \right) \frac{\partial k}{\partial x_j} \right] \quad (5)$$

$$\frac{\partial \epsilon}{\partial t} + U_j \frac{\partial \epsilon}{\partial x_j} = \frac{\epsilon}{k} \left(C_{1\epsilon} \frac{\mu_t}{\rho} S^2 - C_{2\epsilon} \epsilon \right) + \frac{\partial}{\partial x_j} \left[\frac{1}{\rho} \left(\mu + \frac{\mu_t}{\sigma_\epsilon} \right) \frac{\partial \epsilon}{\partial x_j} \right] \quad (6)$$

where S is the strain rate magnitude. In these equations there are 5 free model constants, their standard values are: $C_{1\epsilon} = 1.44$; $C_{2\epsilon} = 1.92$; $C_\mu = 0.09$; $\sigma_k = 1$; and $\sigma_\epsilon = 1.3$.

In our simulation we used COMSOL MULTIPHYSICS program to evaluate airflow distribution in pre-designed container. Boundary conditions are as following: inlet velocity is 8 m/s which is equivalent to the cooling unit capacity 5480 m³/hr at 50 Hz power supply. Turbulence intensity (I) is set to 3%. This value is estimated from the experimental airflow measurements mentioned in Subsection 3.2. The turbulence length scale (l) is estimated to be 0.004 m which represents 5% of the channel height of the inlet.

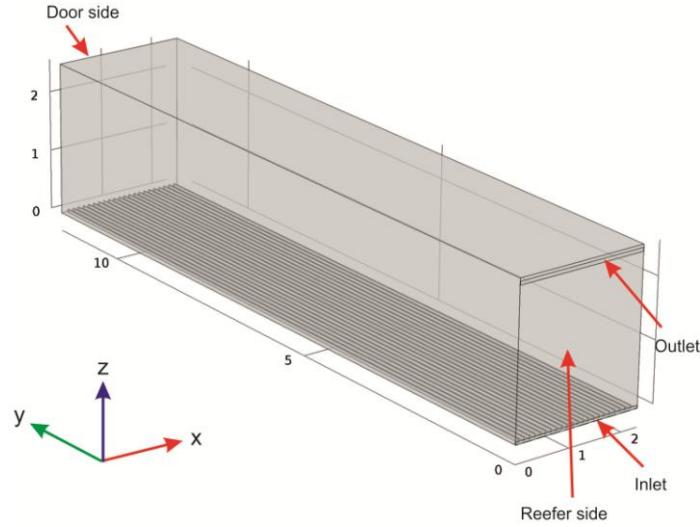


Fig. 1 Empty container

The inner dimensions of the cargo hold of a standard 40 feet reefer container are as follows: 11.590 m for length; 2.294 m for width; and 2.557 m for height. This container is equipped with a Thermoking Magnum Plus cooling unit. Inlet and outlet are at the bottom and top of the reefer side, respectively, as shown in Figure 1. Airflow pattern were extracted for loaded container with banana pallets. One pallet consists of 48 banana boxes, distributed into 8 layers (tiers) 6 boxes in each.

Dimensions of one box are: $0.5 \times 0.4 \times 0.25 \text{ m}^3$. The standard scheme (L1) of pallets layout inside the container is shown in Figure 2 (left). A new layout, called also chimney layout (L2) is tested in our simulations and measurements. In this new layout a considerable gap is created between each four pallets as in Figure 2 (right).

In order to be in accordance with the experimental setup, simulations were done for a reduced number of pallets in the container; 11 for L1 and 12 for L2 (see Figure 2). This difference in pallet number is to obtain approximately aligned ending of the two rows in both layouts. In order to separate the pallets from the unused space in the container, a mobile wall was installed behind the last row of pallets and air sealed by using foam and duct tape.

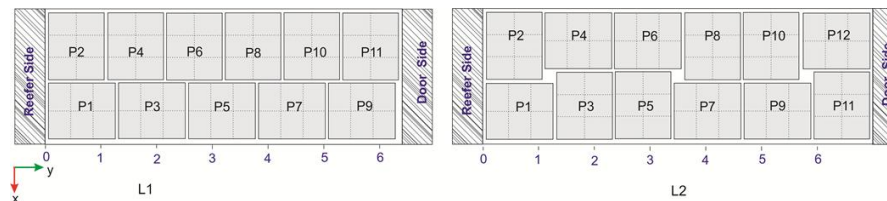


Fig. 2 Top view of the container for both layouts L1 (left) and L2 (right)

Simulations for the two layouts were achieved. We assumed that free convection is negligible since the maximum recorded temperature difference is about 2°C . To show these results in a comparative way, we consider some particular planes in the container. Firstly, in the XY plane three basic cases are essential to be discussed: under the pallets, in the pallets level, and above the pallets. In the inlet level, i.e. under the pallets, as shown in Figure 3, we notice high velocities in the front of container which decrease gradually with the y coordinate. Velocity values are about 8 m/s at the inlet level, 4 m/s in the middle, and 2 m/s at the end of the simulated part. All cases show approximately similar results. However, for higher levels, i.e. in pallets level ($z = 0.2$ to 2.2 m), contradictory results were found. In the front part of the container very low air velocities less than 0.2 m/s at reefer side and then they increase gradually to be about 1 m/s at the middle of the container, and about 3 m/s at the end of the container (see Figure 4). Chimneys don't have identical impact on airflow distribution. Chimney near reefer side has lower velocity values than the one in the middle, which in turn has less value than the one near the door. In the L2 case, where the top of the chimney is closed, we notice how airflow is forced to flow in the gaps surrounding the chimneys (Figure 4 L2). This causes a more uniform distribution of air velocity in L2 layout comparatively with L1 layout.

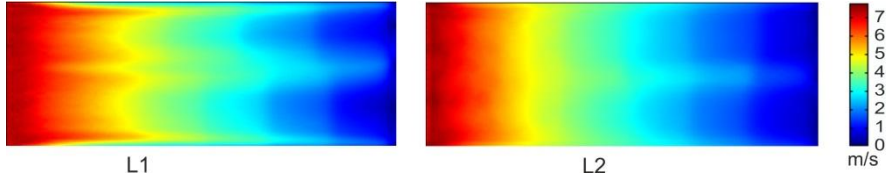


Fig. 3 Airflow pattern in the inlet level for both layouts: L1 and L2.

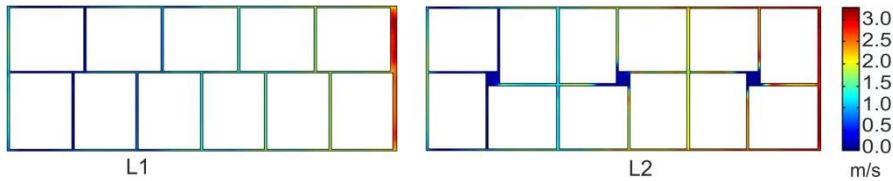


Fig. 4 Airflow pattern in pallets level for both layouts: L1 and L2.

Third level is the outlet level, i.e. above the pallets. There, we have similar airflow distribution to the one at the inlet level with the difference in velocity values and homogeneity (see Figure 5). In Figure 5 we notice that the returning airflow starts with low velocities of about 0.5 m/s and increases gradually to about 3 m/s at the outlet level in reefer side. It is distinguishing that there are two separated clouds of velocity above the two rows of pallets in L1 case. However, for the L2 case we notice a uniform velocity distribution above the first half of the container where the two clouds are merged together for this region and start to separate in the second half. The previous Figures 3 to 5 show that the expected hot spots can be created in the first part of the container. Because the cooling air is supplied from the floor side, the best cooling is achieved in the lowest tier 1. The highest tier 8 is additionally cooled over its top side from the return air flow. The highest temperatures were found in tiers 5 to 7 according to our temperature measurements (Jedermann et al., 2013). Therefore, the boxes in these tiers of the first two pallets are the most likely to produce hot spots. L2 produces, comparatively, the best homogeneity-airflow distribution.

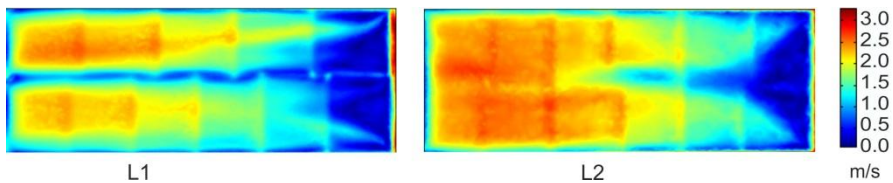


Fig. 5 Airflow pattern above the pallets level for both layouts: L1 and L2.

In the XZ plane, airflow velocity distribution is highly influenced by the y coordinate of this plane. We notice that velocity, in the pallets level, increases with the y coordinate. Highest values are at the end of the container especially in the gap between the door and the last row of pallets. By comparing the velocity distribution at that gap, we find different behavior between L1 and L2 as shown in Figure 6. In

this case, there is non-symmetric distribution. This difference is not only because of the different layout but also because of the larger gap of the left side. The two rows of L1 layout do not end at the same coordinate; the maximum difference is about 4 cm.

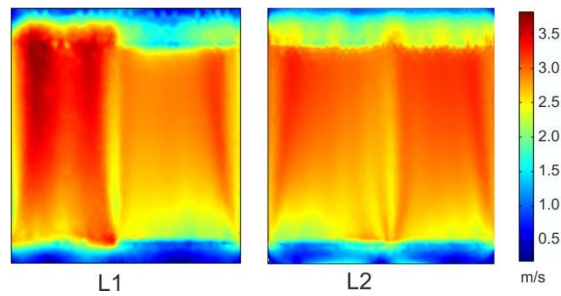


Fig. 6 Comparison between airflow distribution in the XZ plane at the end of the container in the gap between the end pallets and door

The hot spot detected by temperature measurements and proved by the simulation can be explained by the existence of a big eddy in the region near the cooling unit. Figure 7 shows airflow simulation in the YZ-plane in the gap between the two rows of pallets in the standard scheme L1. This explains also the highest temperature values in this region. Changing the layout to the chimney scheme participate in limiting this phenomena and increase the velocity in this region as shown in Figure 8.

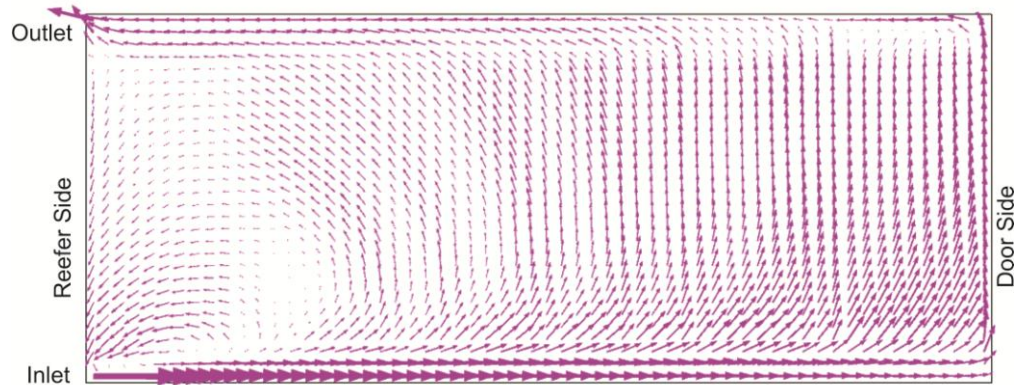


Fig. 7 Airflow pattern in the YZ-plane in gap between the two rows of pallets of L1

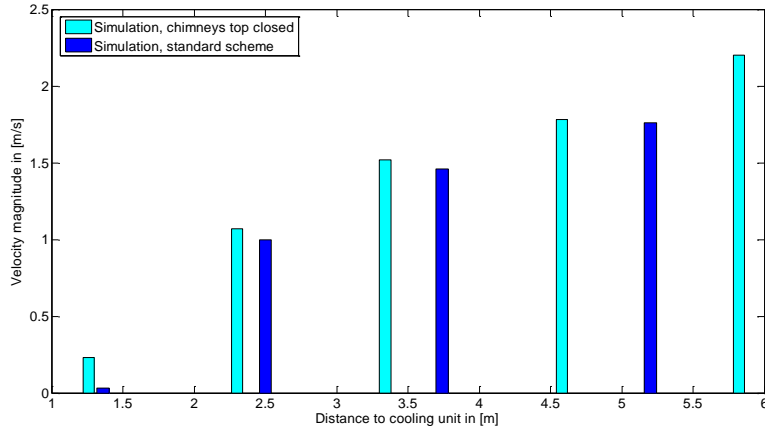


Fig. 8 Average velocity in gaps by simulations

As we see from Figure 8 that the chimney layout improves the airflow distribution inside the container in comparison with the standard scheme layout. However, for both layouts velocity values in the first part of the container still small between the pallets. An idea may increase the velocity in this area is by construction tube in-takes at the bottom of the first chimney, in such a way we force airflow to go in the vertical direction. In this way, we can decrease the entrainment effect which causes the big eddy near the cooling unit. This idea needs to be validated by both simulation and measurement.

3 Evaluation and Conclusions

In order to evaluate simulation results, we made some experimental measurements within the Intelligent Container Project. We used flow sensors based on the thermal principles in these measurements. These sensors include hot-wire anemometers in addition to the IMSAS airflow sensors (Lloyd et al. 2013). In this context we cite one example of the experimental results just to compare it with the simulation results. Figure 9 shows a comparison between the simulation model and experimental results. It is in the floor level of the container under the pallets (inlet plane). In this level there are no obstacles in front of the flow. Both results show a good agreement. Maximum error is about 0.5 m/s which is consider quite good taking into consideration the high turbulence flow inside the container.

As conclusions, simulation of airflow in a logistic container is achieved by this work. Simulation results enable understanding airflow distribution which allows predicting the most likely positions of hot spots in the container. Consequently, taking corrective and preventive actions to maintain the quality of produce and reduce loss rate. Simulations were done by a $k-\epsilon$ turbulent flow model based on

COMSOL simulation program. Results explain some phenomena such as the existence of hot spots near the cooling unit. It proved that the recently introduced scheme of pallets, the “chimney layout”, improves cooling inside the container and gives better airflow distribution.

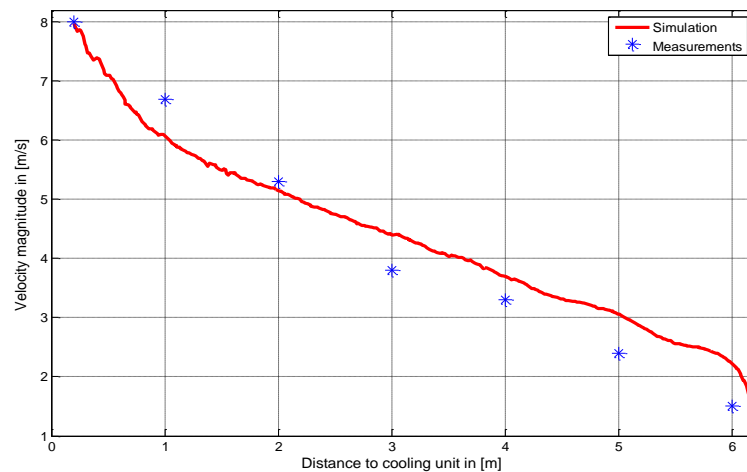


Fig. 9 Comparison between simulation and measurement for velocity magnitudes in the inlet level.

Acknowledgments

The research project “The Intelligent Container” is supported by the Federal Ministry of Education and Research, Germany, under the reference number 01IA10001.

References

- Paull, R., Effect of temperature and relative humidity on fresh commodity quality. *Postharvest Biology and Technology* 1999, 15 (3), 263-277.
- Smale, N. J.; Moureh, J.; Cortella, G., A review of numerical models of airflow in refrigerated food applications. *International Journal of Refrigeration* 2006, 29 (6), 911-930.
- Moureh, J.; Tapsoba, S.; Derens, E.; Flick, D., Air velocity characteristics within vented pallets loaded in a refrigerated vehicle with and without air ducts. *international journal of refrigeration* 2009, 32, 220-234.

Jedermann, R.; Geyer, M.; Praeger, U.; Lang, W., Sea transport of bananas in containers – Parameter identification for a temperature model. *Journal of Food Engineering* 2013, 115 (3), 330-338.

Zou, Q.; Opara, L. U.; McKibbin, R., A CFD modeling system for airflow and heat transfer in ventilated packaging for fresh foods. *Journal of Food Engineering* 2005, 77, 1048–1058.

Xie, J.; Qu, X.-H.; Shi, J.-Y.; Sun, D.-W., Effects of design parameters on flow and temperature fields of a cold store by CFD simulation. *Journal of Food Engineering* 2006, 77 (2), 355-363.

Nieuwstadt, F. T. M.; Eggels, J. G. M.; Janssen, R. J. A.; Pourquié, M. B. J. M., Direct and large-eddy simulations of turbulence in fluids. *Future Generation Computer Systems* 1994, 10 (2–3), 189-205.

Zhai, Z. J.; Zhang, Z.; Zhang, W.; Chen, Q. Y., Evaluation of Various Turbulence Models in Predicting Airflow and Turbulence in Enclosed Environments by CFD: Part 1—Summary of Prevalent Turbulence Models. *HVAC&R Research* 2007, 13 (6), 853-870.

Lloyd, C; Issa, S; Lang, W; Jedermann, R., Empirical airflow pattern determination of refrigerated banana containers using thermal flow sensors. In: *The Intelligent Container, Cool-chain-Management, 5th International Workshop*, University of Bonn, Bonn, June, 2013.